Numerical Winglet Optimization

Neal J. Pfeiffer*
Raytheon Aircraft Company
Wichita, KS

Abstract

A method is presented to optimize the orientation of a winglet on a wing and include the effects of profile drag in addition to induced drag. The method uses the output from four potential-flow solutions in the Trefftz plane well behind the lifting surfaces. The four solutions are a baseline, an angle-of-attack increment, an increment in the root incidence of the winglet, and an increment in the tip incidence of the winglet. Results for the case studied show small differences in the root and tip incidences between an induced-drag-only solution and one with profile drag included.

Nomenclature

Cdp	local-section, profile-drag coefficient
Cdp_o	local-section, parasite-drag coefficient
CDp	aircraft, profile-drag coefficient
CDp_o	aircraft, profile-drag coefficient for baseline case
Chord	local-section chord
Cl	local-section, lift coefficient
Cl_{off}	local-section, lift coefficient for minimum drag
dic	induced-drag, influence coefficients
dic_o	induced-drag, influence coefficients based on the baseline case
ds	differential length along the wake curve in the Trefftz plane
$D_{induced}$	vortex-induced drag
D_o	vortex-induced drag of the baseline case
DICp1	profile-drag, influence coefficients for the first power of the design variables
DICp2	profile-drag, influence coefficients for the second power of the design variables
i	spanwise index
j,k	design-variable indices
K	local-section, induced-drag coefficient
lic	lift influence coefficients
$L_{con.}$	lift constraint
L_o	lift of baseline case
V_∞	freestream velocity
w	velocity component normal to wind axis at the wake in the Trefftz plane
x	design variable
–	local jump in potential across the wake
–	density

* Raytheon Engineering Fellow & Manager New Product Development, AIAA Associate Fellow

Introduction

Winglets have been used on aircraft as a means of reducing the induced drag of the wing, while incurring a reduced structural penalty over a simple span extension. They have been used on a wide range of airplanes, from general aviation through transport aircraft. They have also been designed as add-on devices for existing airplanes and more now as part of the basic design.

The initial concept for the winglet was developed experimentally. Wind-tunnel and flight tests were run to evaluate the effects of shape, size, and orientation of winglets. Databases were constructed from the results of these tests and used for the early winglet designs.

Computational methods were used to analyze winglet configurations for a range of size, shape, and orientation. They were then used with optimization techniques to more efficiently design winglets. Most of these methods utilized a Trefftz-plane analysis of the wake downstream of the airplane to guide the design.

While the Trefftz-plane method addresses a major drag component, induced drag, it neglects a secondary one, profile drag. The variation in profile drag needs to be understood in order to minimize the total drag of the configuration with the winglet. A model for profile drag is proposed and incorporated with an induced-drag optimization method for winglet orientation on an existing wing.

This study was initially undertaken to evaluate a published, induced-drag, optimization technique and modify it to include the effect of parasite drag. This would be used in the early stages of a winglet design. While this was accomplished, it uncovered a number

of interesting details and pointed to other work to be done.

Background

The initial work with winglets was done by Richard Whitcomb at NASA. In 1976 he presented a design approach for winglets [1] that involved the use of vortex-lattice methods along with parametric experimentation in the wind tunnel. Also in 1976, Kichio Ishimitsu from Boeing wrote an AIAA paper [2] on the design and analysis of winglets. This paper had theoretical and experimental results for winglets on a KC-135 airplane.

In a 1984 paper, Ilan Kroo outlined a method to design optimally-loaded, lifting surfaces [3] using a discrete-vortex, Weissinger technique. A more recent paper [4] by Steve Smith from NASA Ames described the use of potential flow calculations, along with the basic Kroo technique, to design winglets in order to minimize the induced-drag of a transport aircraft.

Another area of winglet research has focused on competition sailplanes. It would seem that the use of winglets would have come quickly to the sailplane community where several of the classes have specific limits on wingspan. Yet it did not happen that way. The early attempts at winglets did significantly reduce the induced drag and improve climb performance and cruise at moderate speeds, however, at higher speeds this induced-drag reduction was overcome by the added parasite drag caused by the added winglet surfaces. The use of laminar-flow, airfoil sections made this particularly noticeable. This balance between induced and parasite drag meant that while a first-generation, racing sailplane with winglets could climb and cruise at lower speeds better than one without winglets, the pilot with winglets would have more drag and a higher sink rate than a competitor without winglets, when flying fast between thermals. This was not acceptable for a competitor trying to fly a cross-country task at the highest speed. Because of this, sailplane designers learned that it was not enough to design only for minimum induced drag, which gave big benefits at low speed. Instead they realized that it was important to also include the effects of parasite drag in the optimization so that the sailplane with winglets would always have some benefit over one without. Mark Maughmer at Penn State University has written a paper [5] that discusses the design process for modern sailplane winglets.

It is interesting though, that the original references for winglets realized the need for minimizing the total drag, not just the induced portion. The following excerpt is from reference 1.

> *The theories of references 3, 7, and 9 indicate that to achieve the reductions in induced drag theoretically predicted for wing-tip mounted vertical surfaces requires not only substantial inward loads on these surfaces but also significant increases in the upward loads on the outboard region of the wing. Exploratory experiments made both during the investigation of reference 4 and during the present investigation indicate that the greatest measured reductions in drag due to adding the upper winglet are achieved with normal loads on the winglet, and associated added loads on the outboard region of the wing, substantially less than those indicated as optimum by the theories of references 3, 7, and 9. These differences are probably due primarily to viscous effects not included in theory. Calculations based on reference 9 indicate that reducing these loads from the theoretical optimum values to the measured values decreases the effectiveness of the winglets only slightly (induced drag increases slightly). This effect is probably more than offset by a reduction in viscous drag for both the winglet and the wing resulting from lower induced velocities on these surfaces at the lower load condition.*

Similarly, from reference 2,

> *A change in the wing parasite and compressibility drag occurs when winglets are added to a configuration. These drag changes are due to the changes in the pressure and loading distributions that accompany the winglet addition. These drag increments are estimated using wind tunnel data of the base configuration and the changes in lift curve slope calculated from the theoretical analysis. Account must be made of the increase in parasite drag and compressibility drag on the outboard wing due to the higher velocities induced by the winglet.*

And from reference 3,

> *It is important to include viscous drag in the determination of optimal load distribution. Since profile drag varies with lift coefficient, the inclusion of this term precludes extremely*

high section lift coefficients which might otherwise appear on planforms with small tip chords.

The comments from these references all point to the importance of the 2D drag of the airfoil sections for the wing and winglet in addition to the induced terms due to a finite span. If the winglet is optimized on induced, trailing-vortex drag alone so that the winglet load is high, it can cause the profile drag of the airfoils sections along the outboard wing and winglet to be too large. This is particularly true if laminar-flow airfoils are used with a highly-loaded winglet, which causes the drag of the airfoil sections to move out of their laminar buckets. If on the other hand, a more moderately-loaded winglet is used, there will still be a significant reduction in the induced, trailing-vortex drag, but the profile drag will be significantly lower and will provide a better solution, especially at higher cruise speeds. The primary design point also needs to be chosen carefully. If the point is chosen at a long-range-cruise speed at high altitude, it may actually reduce the maximum speed of the aircraft at mid altitudes. If the high-speed point is used it will likely reduce the range slightly for long-range-cruise speed. The designer should examine both and choose one, or a compromise solution in between.

Existing Induced-Drag Method

The method presented by Steve Smith [4] provided a means to optimize the orientation of a winglet on an existing wing by minimizing the induced drag at a downstream Trefftz plane. The method utilizes the local circulation and downwash values from a potential-flow analysis. These values are calculated at many points spanwise along the wake well downstream of the wing and winglet. It then integrates the influence of the wake columns on each other to predict the lift and drag. The influence coefficients for drag are then integrated with respect to three design variables; the root incidence of the winglet, the tip incidence of the winglet, and the angle of attack of the wing-winglet combination. The variation in angle of attack is required so that the optimization can be done at constant aircraft lift.

A quadratic expression for induced drag is developed in terms of the design variables, {x}.

$$D_{induced} = \{x\}^T [dic] \{x\} + \{dic_o\}^T \{x\} + D_o \qquad (1)$$

Where the induced-drag, influence coefficients are defined by

$$[dic]_{jk} = \rho \sum_i \frac{\partial \mu_i}{\partial x_j} \frac{\partial w_i}{\partial x_k} ds_i \qquad (2)$$

and

$$\{dic_o\}_j = \rho \sum_i \left(\mu_{oi} \frac{\partial w_i}{\partial x_j} + w_{oi} \frac{\partial \mu_i}{\partial x_j} \right) ds_i \qquad (3)$$

The summations integrate the spanwise influences across i, and the j and k indices are both for the design variables of x.

The derivative of the drag equation is then used to find the optimum values for the design variables. This equation for minimum induced drag can be written:

$$[dic + dic^T]\{x\} = -\{dic_o\} \qquad (4)$$

The following lift equation is used as the basis for a constraint on wing lift.

$$Lift = \{lic\}^T \{x\} + L_o \qquad (5)$$

Where the lift influence coefficients are defined by:

$$[lic]_j = 2\rho \sum_i \frac{\partial \mu_i}{\partial x_j} dy_i \qquad (6)$$

By using the lift equation and a Lagrange-augmented cost function, the optimization problem for induced drag is reduced to the following matrix equation.

$$\begin{bmatrix} dic + dic^T & | & lic \\ - - - - & & - \\ lic & | & 0 \end{bmatrix} \begin{Bmatrix} x \\ - \\ \lambda \end{Bmatrix} = \begin{Bmatrix} -dic_o \\ - - - \\ Lcon. - L_o \end{Bmatrix} \qquad (7)$$

Method to Characterize Profile Drag

Up to this point, the only drag that is has been calculated is that due to the influence of the wake sheet of the finite wing. The profile drag of the wing, which consists of the skin friction on the wing surface and the form drag of the airfoils along the wing, has not been included. Skin friction will be nearly constant for the typical design variables of winglet incidence and twist (unless laminar flow is an issue), but would be important if winglet planform was varied. The form drag, however, is always important. The variation of form drag for the winglet and outer wing can easily be of the same magnitude as the variation of induced drag for the wing and winglet combination with changes in loading due to incidence and twist. For transonic applications, the variation in form drag with lift is doubly important since increased loading can easily cause unwanted compressibility drag. Thus it is important to have a means to calculate the profile drag along the wing and winglet and then combine it with the induced drag component to have a full optimization.

The local section profile drag is composed of two parts; a constant, plus a part that is dependent on the

square of a local lift term. For strip 'i' along the wing, the profile drag coefficient is:

$$C_{dp(i)} = C_{dpo(i)} + k_{(i)} \left(C_{l(i)} - C_{loff(i)}\right)^2 \quad (8)$$

where the C_{loff} term is the section lift coefficient for minimum profile drag. Now inserting the above relationship for section drag gives:

$$C_{dp(i)} = C_{dpo(i)} + k_{(i)} \left(\frac{2\mu_{(i)}}{Chord_{(i)} V_\infty} - C_{loff(i)} \right)^2$$

$$= C_{dpo(i)} + k_{(i)} \left(\frac{4\mu_{(i)}^2}{Chord_{(i)}^2 V_\infty^2} - \frac{4\mu_{(i)}}{Chord_{(i)} V_\infty} C_{loff(i)} + C_{loff(i)}^2 \right) \quad (9)$$

Now incorporate the design variables into the μ term using the first term of a Taylor-series expansion.

$$C_{dp(i)} = C_{dpo(i)} + k_{(i)} \left(\begin{array}{l} \frac{4}{Chord_{(i)}^2} \left(\frac{\mu_{i(o)}}{V_\infty} + \sum_{j=1}^{m} \frac{\partial \mu_i / V_\infty}{\partial x_j} \delta x_j \right)^2 \\ - \frac{4}{Chord_{(i)}} \left(\frac{\mu_{i(o)}}{V_\infty} + \sum_{j=1}^{m} \frac{\partial \mu_i / V_\infty}{\partial x_j} \delta x_j \right) C_{loff(i)} \\ + C_{loff(i)}^2 \end{array} \right) \quad (10)$$

These section coefficients can then be summed across all of the spanwise columns to find the total contribution from profile drag. This results in the following matrix equation.

$$CDp = CDpo + \{DICp1\}^T \{x\} + \{x\}^T [DICp2] \{x\} \quad (11)$$

The first term is independent of the design variables. The second term is a function of the first power of the design variables, and given three design variables, can be written in the following vector form. These equations are calculated in typical drag coefficient form with the variable 'sym' equal to two for a symmetric wing about a vertical center plane.

$$\{DICp1\}^T \{x\} = \frac{4(sym)}{V_\infty^2 S} \begin{Bmatrix} \sum_{i=1}^{n} k_{(i)} \left(\left(\frac{2\mu_{i(o)}}{Chord_{(i)}} - V_\infty C_{loff(i)} \right) \frac{\partial \mu_i}{\partial x_1} \right) ds_{(i)} \\ \sum_{i=1}^{n} k_{(i)} \left(\left(\frac{2\mu_{i(o)}}{Chord_{(i)}} - V_\infty C_{loff(i)} \right) \frac{\partial \mu_i}{\partial x_2} \right) ds_{(i)} \\ \sum_{i=1}^{n} k_{(i)} \left(\left(\frac{2\mu_{i(o)}}{Chord_{(i)}} - V_\infty C_{loff(i)} \right) \frac{\partial \mu_i}{\partial x_3} \right) ds_{(i)} \end{Bmatrix}^T \begin{Bmatrix} \delta x1 \\ \delta x2 \\ \delta x3 \end{Bmatrix} \quad (12)$$

Similarly, the matrix in equation (11) with the squared terms can be written as:

$$[DICp2] = \begin{bmatrix} \sum_{i=1}^{n} \frac{k_{(i)}}{Chord_{(i)}} \left(\frac{\partial \mu_i}{\partial x_1} \right)^2 ds_{(i)} & \sum_{i=1}^{n} \frac{k_{(i)}}{Chord_{(i)}} \left(\frac{\partial \mu_i}{\partial x_1} \frac{\partial \mu_i}{\partial x_2} \right) ds_{(i)} & \sum_{i=1}^{n} \frac{k_{(i)}}{Chord_{(i)}} \left(\frac{\partial \mu_i}{\partial x_1} \frac{\partial \mu_i}{\partial x_3} \right) ds_{(i)} \\ \sum_{i=1}^{n} \frac{k_{(i)}}{Chord_{(i)}} \left(\frac{\partial \mu_i}{\partial x_1} \frac{\partial \mu_i}{\partial x_2} \right) ds_{(i)} & \sum_{i=1}^{n} \frac{k_{(i)}}{Chord_{(i)}} \left(\frac{\partial \mu_i}{\partial x_2} \right)^2 ds_{(i)} & \sum_{i=1}^{n} \frac{k_{(i)}}{Chord_{(i)}} \left(\frac{\partial \mu_i}{\partial x_2} \frac{\partial \mu_i}{\partial x_3} \right) ds_{(i)} \\ \sum_{i=1}^{n} \frac{k_{(i)}}{Chord_{(i)}} \left(\frac{\partial \mu_i}{\partial x_1} \frac{\partial \mu_i}{\partial x_3} \right) ds_{(i)} & \sum_{i=1}^{n} \frac{k_{(i)}}{Chord_{(i)}} \left(\frac{\partial \mu_i}{\partial x_2} \frac{\partial \mu_i}{\partial x_3} \right) ds_{(i)} & \sum_{i=1}^{n} \frac{k_{(i)}}{Chord_{(i)}} \left(\frac{\partial \mu_i}{\partial x_3} \right)^2 ds_{(i)} \end{bmatrix} \quad (13)$$

or the entire term with design variables:

$$\{x\}^T [DICp2] \{x\} = \frac{4(sym)}{V_\infty^2 S} \begin{Bmatrix} \delta x1 \\ \delta x2 \\ \delta x3 \end{Bmatrix}^T [DICp2] \begin{Bmatrix} \delta x1 \\ \delta x2 \\ \delta x3 \end{Bmatrix} \quad (14)$$

Differentiating this profile-drag equation with respect to these design variables gives the following equation.

$$\frac{d}{dx} CDp = \{DICp1\}^T + \left[DICp2 + DICp2^T \right] \{x\} \quad (15)$$

Assemble the New Model

The induced and profile drag terms are combined in the following matrix equation to optimize for the total drag at a constrained lift.

$$\left[\begin{array}{c|c} dic + dic^T + dic_{p2} + dic_{p2}^T & lic \\ \hline lic & 0 \end{array} \right] \left\{ \begin{array}{c} x \\ \hline \lambda \end{array} \right\} = \left\{ \begin{array}{c} -dic_o - dic_{p1} \\ \hline Lcon. - L_o \end{array} \right\} \quad (16)$$

It is important to insure that the terms for induced and profile drag have the same dimensional or non-dimensional level so their relative weights are preserved.

Procedure

Analysis has been made with linear-potential code, VSAERO at a high, subsonic Mach number. Typical surface pressure results and trailing wake filaments are shown in Figure 1.

The intent of this study was to maintain the same trailing-edge points and wake shape for the analysis of all of the cases. This eliminated any mixing of the rotation of winglet sections with changes to the wake shape. It was felt that this would give the pure effects of section rotation.

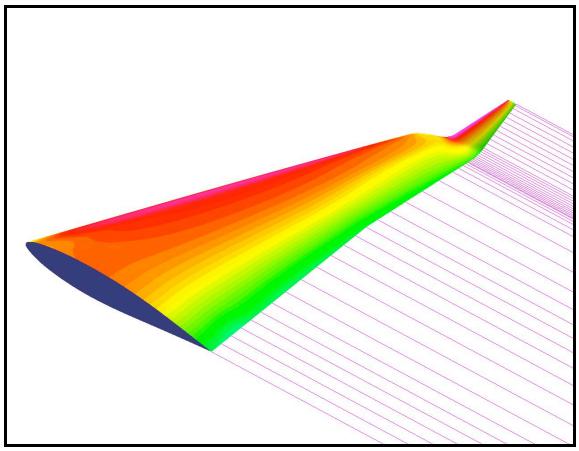

Figure 1 Typical wing and winglet combination with trailing wake

The geometry definition for the VSAERO program makes it convenient to model parametric variations in orientation. Airfoil sections are defined on the winglet and the transition from the wing. The orientation of these defining sections is set by entering an angular rotation value at the trailing edge for each section cut. This makes the changing of the local orientation of the geometry relatively simple and quick.

The airfoils on the transition region, between the wingtip and root of the winglet, are defined in a computer-aided-design (CAD) system on equally spaced planar cuts through this region (see Figure 2.) These planes are oriented streamwise and the rotation angle between each adjacent plan is equal. The winglet is defined by a root and a tip section that lie in parallel planes. Rotation points are defined at the trailing edge of the rib airfoils on the transition and winglet. A rotation line for each of these sections is defined through the trailing-edge point and perpendicular to the plane of the rib.

A swept wing and winglet with a fixed planform were used for this study. The baseline geometry had zero incidence at the root of the winglet and 2-degrees of toe-out at the tip. The only geometric change was to the orientation of the winglet, including the transition from the wing tip. The first of two geometric changes was a 1–degree increment in incidence at the root of the winglet, with smooth, linear variation of twist in the transition from the wing to the winglet and linear transition from the root to the baseline incidence at the tip. The second geometric change was a 1-degree increment in incidence at the tip of the winglet, with linear variation back to the baseline incidence at the winglet root. The superposition of these increments, along with the baseline and alpha cases, allowed the optimization program to produce the optimal incidence and twist of the winglet for a specific flight condition.

VSAERO was run for a baseline case, a case with an increment in angle of attack, a case with an increment in root incidence of the winglet, and a case with an increment in the tip incidence of the winglet. The Trefftz-plane results for these runs were extracted from the four output files and used to feed the optimization program.

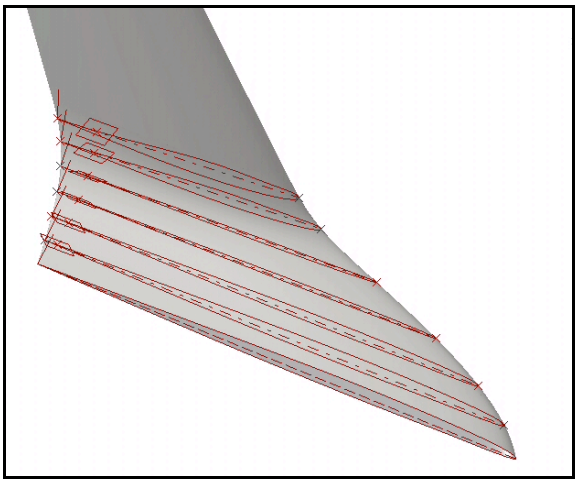

Figure 2 View of winglet with section cuts

Two-dimensional drag polars were estimated for each of the airfoil sections used in the VSAERO, Trefftz-plane calculations. A simple parabola with lift offset for minimum drag was used. A separate file that characterized the drag polars and chord lengths of the airfoil sections of the wing and winglet was used by the optimization program to determine the influence of the parasite drag.

Results

Results are presented for a Mach = 0.70 condition which would correspond to a long-range-cruise speed for many business jets. Business jets tend to have a lower wing loading than transport aircraft and thus have a lower design lift coefficient. Even so, at Mach = 0.70, the use of VSAERO is at its limits. For a C_L of 0.35 to 0.40, the suction peaks at the leading edge are just at or slightly above the sonic level. Any higher Mach number or loading would require the use of a full-potential method. But since goal of this study was to investigate the basic technique and the relative sensitivity of the induced and parasite

portions of the drag, the ability to make rapid runs was considered important enough to use the simpler method.

The optimized winglet incidence and twist for a lift coefficient of 0.35 are shown in Table 1. The first part of the table shows the results for inviscid VSAERO analysis. The effect of induced-drag-only versus total-drag optimization shows a small shift in the root incidence of about two-tenths of a degree. The results in the bottom half of the table are for VSAERO runs with boundary layers on surface streamlines that have been iterated ten times with the potential flow solution. Again, the incidence difference between induced-drag-only and total-drag optimization is again about two-tenths of a degree at the root. However, there are shifts in both root and tip incidences between the inviscid and viscous solutions that yield about three-tenths of a degree total difference in winglet twist. This is caused by the changes to spanload due to the boundary layer.

Optimization Type	Root Incidence (deg)	Tip Incidence (deg)	Winglet Twist (deg)
Inviscid VSAERO			
Induced-Drag Only	2.21	-2.66	-4.87
Total Drag	1.99	-2.67	-4.66
Viscous VSAERO			
Induced-Drag Only	2.42	-2.12	-4.54
Total Drag	2.23	-2.13	-4.36

Table 1 Optimization results for CL = 0.35

At higher Mach numbers, viscous effects will cause a movement of the chordwise location of a shock on the wing. This will change both the spanload and the normalwash to a greater degree than noted for this case.

The use of viscous results must be monitored, however, to avoid the introduction of noise into the Trefftz-plane calculations. If a boundary-layer calculation indicates the possibility of separation before reaching the trailing edge, it is best if there is an ability to simulate a displacement thickness for a thin separation. This will make the spanload results smoother and cause fewer problems with the calculation of normalwash, which depends on the derivative of the local circulation. The older, integral-boundary-layer routines within VSAERO could produce significant wiggles in the downwash distribution. The newer, boundary-layer option reduces or eliminates these wiggles and provides smoother spanload distributions. The results in the next two tables were made without boundary layers in order to eliminate a secondary source of noise.

The optimization results for winglet orientation at a higher lift coefficient are shown in Table 2. These show an increase in root angle of about four-tenths of a degree and an increase at the tip of about two-tenths of a degree, when compared with the results in Table 1. This causes a net increase in twist of about two-tenths of a degree for the higher lift coefficient.

Optimization Type	Root Incidence (deg)	Tip Incidence (deg)	Winglet Twist (deg)
Inviscid VSAERO			
Induced-Drag Only	2.61	-2.46	-5.07
Total Drag	2.40	-2.47	-4.87

Table 2 Optimization results for CL = 0.40

As a check of the method, new runs were made using a different baseline geometry that is closer to the optimized shape for the lift coefficient of 0.35 above. The new geometry used a root incidence of +2.0 degrees (toe in) and a tip incidence of –2.0 degrees (toe out). The optimization results for this new baseline are shown in Table 3. The largest variation between the optimized incidences for the new and old baseline geometries is only 0.17 degree and the variation in twist is only 0.18 degree.

Optimization Type	Root Incidence (deg)	Tip Incidence (deg)	Winglet Twist (deg)
Inviscid VSAERO			
Induced-Drag Only	2.35	-2.56	-4.91
Total Drag	2.16	-2.68	-4.84

Table 3 Optimization results for CL = 0.35 with a new baseline having a root incidence of +2 deg and a tip incidence of –2 deg

Conclusions

This method is an extension of the existing Smith method and is relatively simple and quick. It is intended to be a method that could be applied early in the development process with the use of a linear-potential, panel method.

For the optimization of winglet twist for a business aircraft without laminar flow and for long-range-cruise speeds, the effects of profile drag are secondary. The presence of either laminar flow or mild to moderate shocks at higher speeds will make the inclusion of profile drag more important.

The speed of this method allows it to be used to estimate optimum, winglet orientation for a range of lift coefficients using the same four potential-flow runs. This is important when looking at the usefulness of the entire design. It would require new runs for additional Mach numbers, however, the basic geometry in these runs would remain unchanged. Optimizations can be run quickly for a range of Mach and CL conditions and allow the designer to better understand how much the optimal orientation will vary. A best compromise can then be chosen, given the aircraft requirements.

This method only addresses a portion of the winglet problem, its orientation. The other significant portion is the optimization of the size and shape of the winglet. The parametric capabilities of modern CAD programs should be employed to define an arbitrary winglet. By varying the parameters for winglet height, chords, and sweep, the size and shape of the winglet could be mathematically defined and rapidly changed for a panel-code analysis. This variation of shape and size will make the inclusion of profile drag more important, since the wetted area becomes a variable.

References

1. Whitcomb, Richard T., "A Design Approach and Selected Wind-Tunnel Results at High Subsonic Speeds for Wing-Tip Mounted Winglets," NASA TN D-8260, June 1976.
2. Ishimitsu, K. K., "Aerodynamic Design & Analysis of Winglets," AIAA Paper 76-940, Sept. 1976.
3. Kroo, Ilan, "Design and Analysis of Optimally-Loaded Lifting Systems," AIAA Paper 84-2507, Oct. 1984.
4. Smith, Stephen C., "Trefftz-Plane Drag Minimization at Transonic Speeds," SAE Paper 971478, April 1997.
5. Maughmer, Mark D., "The Design of Winglets for High-Performance Sailplanes," AIAA JOA, Nov.-Dec. 2003, based on AIAA Paper 2001-2406, June 2001

Acknowledgements

I would like to thank Steve Smith for his numerous consultations over the phone and by email. I would like to thank David Aronstein, Juan Alonso, and John Gallman for conversations that helped me deal with the data. I also thank my wife, Karen, and son, Kevin, for proofreading.